

Tight-binding Theoretical Study of Band Gap Opening in Graphene

S SAHU¹ and G.C. ROUT²

¹School of Applied Sciences (Physics), Campus-3, KIIT University, Odisha, India

²Physics Enclave, PlotNo.- 664/4825, Lane-4A, Shree Vihar, Chandrasekharpur, PO-Patia, Bhubaneswar- 751024, Odisha, India

Received: 10.11.2014 ; Accepted : 15.1.2015

Abstract. We report here the tight-binding model calculation for tuning the band gap in semimetallic graphene near Dirac point by various interactions. We propose a model Hamiltonian consisting of hopping of electrons up to third nearest-neighbors, substrate effect, Coulomb interaction, electron-phonon interaction and high frequency phonon vibrations and finally the bilayer graphene. We calculate physical parameters by Green's function technique and investigate the band gap opening due to different approach.

Keywords. Graphene, Coulomb interaction, electron-phonon interaction, bilayer graphene

PACS Nos. 81.05.ue., 73.22.pr, 72.80.Vp

1. Introduction

Graphene is a one-atom-thick two dimensional structure with carbon atoms packed in a honeycomb lattice. Its recent experimental discovery has stimulated extensive investigations on every aspects of this novel material [1, 2]. The tight-binding calculation for graphene shows that its conduction and valence bands touch at six points K and K' (Dirac points) in the Brillouin zone [3] where energy dispersions are linear with respect to momentum. This unique band dispersion in graphene leads to graphene's novel physical and electronic properties such as room temperature quantum Hall effects and high charge carrier mobility [4-6]. Graphene, being a gap-less semi-metal, can not be used in pristine form for nano-electronic applications. Therefore, it is necessary to open a finite gap in the energy dispersions at K points by various mechanisms [7, 8]. Small gaps have been observed, when graphene is placed on substrates such as boron nitride (BN) (100meV) [9] and silicon carbide (SiC) (250 meV) [10]. There is a great effort for enhancing these gaps up to 1eV order of magnitude observed in silicon

/germanium for the applications in digital electronics. The recent work indicates that a carbon layer is co-covalently bonded to the SiC sub-lattice [11-15]. Symmetry breaking has been suggested as the gap opening mechanism for the graphene-on-Ruthenium system [16]. McCann and Falco [8, 17] have proposed that bilayer graphene can develop a gap, when it is gated with an electric field. Bilayer graphene gap has been observed experimentally by using infrared spectroscopy [18] and angle resolved photo emission spectroscopy (ARPES) [19]. Hague [20, 21] has presented a theoretical model calculation for the strong enhancement of graphene-on-substrates band gaps by attractive interactions mediated through phonon's in polarizable substrates. The band gap of several eV can be prepared by chemical modifications with hydrogen (Graphane) [22] and Fluorine (Fluorographene) [23]. Atomic thick boron nitride (BN) forms a honeycomb lattice where the π orbitals on N sites are shifted up in energy by $+\Delta$ and decreased in energy of $-\Delta$ on B sites causing a gap of 2Δ [24]. The band gap of 5.56 eV is observed experimentally on mono-layer BN systems.

The role of Coulomb interaction in graphene and related systems provides a long standing problem. The two dimensional graphene [25, 26], a number of ad-atoms on semiconductor surfaces such as Si : X (Si, C, Sn, Pb) [27], Bechgard Salts [28] polymers [29, 30] display strong local as well as non-local Coulomb interactions. It is observed that in graphene the on-site Coulomb interaction is $U/t_1 \sim 3.3$ and the near-neighbor Coulomb interactions is $V/t_1 \sim 2$ where t_1 is the nearest neighbor hopping $t_1 = 2.8\text{eV}$ [31]. The effective on-site (Hubbard) interaction is $U = 3.3 t_1$ in graphene in the close vicinity of the critical value separating conducting graphene from an insulating phase [32]. The Coulomb interaction between massless fermions in pristine graphene remains long ranged and unscreened. It is currently unclear whether this would lead to strongly correlated electronic phases like an insulator [33, 35] or whether graphene is rather weakly correlated. The unscreened long-range Coulomb interaction is shown to be responsible for many unusual behaviors in graphene [34, 36]. The local Coulomb interaction is crucial for the theory to understand the defect induced magnetism [37] and Mott transitions on the surfaces like Si:X.

2. Theoretical model

Single layer graphene is formed by carbon atoms arranged in a two-dimensional non-Bravais honeycomb lattice. The distance between nearest-neighbor carbon atoms is $a_0 \approx 1.42\text{\AA}$, while the lattice constant is $a = \sqrt{3} a_0$. The geometry and the 2D-character of the lattice do not allow the overlap of the p_z

orbitals of a given carbon atom and the s, p_x, p_y orbitals of its neighbors. The s, p_x, p_y orbitals hybridize to create sp^2 bonds and form high energy σ bands. The π band is created by the overlap of p_z orbitals in graphene and this band is responsible for electronic properties. A simple tight-binding model incorporating only the nearest-neighbor hopping between adjacent distinct A and B sub-lattices provides a good approximation for studying the low energy electronic excitations and doping in pristine graphene .

Assuming that the electron can hop to both the nearest and next-nearest-neighbor atoms, the tight binding Hamiltonian for electron in graphene can be written as

$$H_0 = \sum_{i,\sigma} (\varepsilon_a a_{i,\sigma}^\dagger a_{i,\sigma} + \varepsilon_b b_{i,\sigma}^\dagger b_{i,\sigma}) - t_1 \sum_{(i,j),\sigma} (a_{i,\sigma}^\dagger b_{j,\sigma} + b_{j,\sigma}^\dagger a_{i,\sigma}) - t_2 \sum_{\langle\langle i,j \rangle\rangle,\sigma} (a_{i,\sigma}^\dagger a_{j,\sigma} + b_{j,\sigma}^\dagger b_{i,\sigma}) - t_3 \sum_{\langle\langle\langle i,j \rangle\rangle\rangle,\sigma} (a_{i,\sigma}^\dagger b_{j,\sigma} + b_{j,\sigma}^\dagger a_{i,\sigma}) \quad (1)$$

where $a_{i,\sigma}^\dagger$ ($a_{i,\sigma}$) create (annihilates) an electron with spin σ ($\sigma = \uparrow, \downarrow$) on site \vec{R}_i sub-lattices A. Similarly $b_{i,\sigma}^\dagger$ ($b_{i,\sigma}$) create (annihilates) an electron on sub-lattices B. Here t_1 ($= 2.5$ to 3.0 eV) is the nearest- neighbor hopping energy, t_2 with $0.02 t_1 \leq t_2 \leq 0.2 t_1$ [36, 37] is the next- nearest- neighbor hopping energy and ε_a (ε_b) is the site energy at the sub-lattice site A(B) . Further $\langle i, j \rangle$, $\langle\langle i, j \rangle\rangle$ and $\langle\langle\langle i, j \rangle\rangle\rangle$ stand for nearest, next-nearest and next-to-next-neighbor hoppings from site \vec{R}_i to \vec{R}_j .

The Fourier transformed dispersion $\gamma_1(k)$ for the nearest neighbor hopping is

$$\gamma_1(k) = e^{ik_x a_0} + 2e^{-i\frac{1}{2}k_x a_0} \cdot \cos \frac{\sqrt{3}}{2} k_y a_0 \quad (2)$$

and the dispersion $\gamma_2(k)$, $\gamma_3(k)$ for the next and next-to-next-nearest-neighbor hopping are $\gamma_2(k) = \sum_{\delta_2} e^{i\vec{k} \cdot \vec{\delta}_2}$, $\gamma_3(k) = \sum_{\delta_3} e^{i\vec{k} \cdot \vec{\delta}_3}$, where $\vec{\delta}_2$ and $\vec{\delta}_3$ are the next-nearest neighbor lattice vector. Graphene deposited on SiO_2 is well described by the 2D massless Dirac equation [3]. Graphene grown on SiC can be described in terms of massive 2D Dirac electron [5] . Substrate induced potential can break the symmetries of the honeycomb lattice and generate gaps in the electronic system. In a graphene-on-substrate system, the electron interacts with

the static potential induced by the substrate. As a result, a modulated potential, where A site have energy $+\Delta$ and B sites with energy $-\Delta$, leads to the breaking of the symmetry between A and B sites and gives rise to a gap. Such a symmetry breaking Hamiltonian is written as

$$H_{sub} = \Delta \sum_{i,\sigma} a_{i,\sigma}^\dagger a_{i,\sigma} - \Delta \sum_{i,\sigma} b_{i,\sigma}^\dagger b_{i,\sigma} \quad (3)$$

This system exhibits a band gap 2Δ and if un-doped, has an insulating ground state with the Fermi level lying in the gap. The effect of Coulomb repulsion is to stop both electrons occupying the same site. The Hamiltonian describing the Coulomb interaction with an effective Coulomb energy U is written as

$$H_U = U \sum_i \left[n_{i\uparrow}^a n_{i\downarrow}^a + n_{i\uparrow}^b n_{i\downarrow}^b \right] \quad (4)$$

where $n_{i\uparrow}^\alpha$ ($n_{i\downarrow}^\alpha$) with $\alpha \in A, B$ sub-lattices, represents the occupation number operator of up(down) spin. For weak coupling, the Hamiltonian can be decoupled by Hartree-Fock mean-field decoupling scheme i.e. $U n_{i\uparrow}^\alpha n_{i\downarrow}^\alpha \approx U \langle n_{i\uparrow}^\alpha \rangle n_{i\downarrow}^\alpha + U \langle n_{i\downarrow}^\alpha \rangle n_{i\uparrow}^\alpha - U \langle n_{i\uparrow}^\alpha \rangle \langle n_{i\downarrow}^\alpha \rangle$ where $\alpha \equiv a, b$ corresponding to A and B site interactions. The mean-field solutions are taken as $(\langle n_{i\uparrow}^a \rangle + \langle n_{i\uparrow}^b \rangle) / 2 = n$ and $(\langle n_{i\uparrow}^a \rangle - \langle n_{i\uparrow}^b \rangle) / 2 = d$ and this leads to the condition, $\langle n_{i\uparrow}^a \rangle = n + d$ and $\langle n_{i\uparrow}^b \rangle = n - d$ where n represents the mean electron occupation and d the deviation from the mean occupation. Similar expression can be formed for the down spin electron. The electron-phonon interaction and lattice vibration are written as

$$H_{e-ph} = \sum_{\alpha,i,j} f(i-j) n_{i,\sigma}^\alpha (b_j^\dagger + b_j) \quad (5)$$

$$H_p = \sum_j \omega_0 b_j^\dagger b_j \quad (6)$$

Here H_{e-p} represents the electron density $n_{i,\sigma}^\alpha$ at sites is coupled to the phonon displacement $u_j = b_j^\dagger + b_j$ with phonon creation (annihilation) operator b_j^\dagger (b_j) at

site j and $f(i-j)$ is the electron-phonon coupling. for high frequency phonon's equations () represents the Holstein interaction .The Hamiltonian H_p represents the free phonon energy with phonon frequency ω_0 .

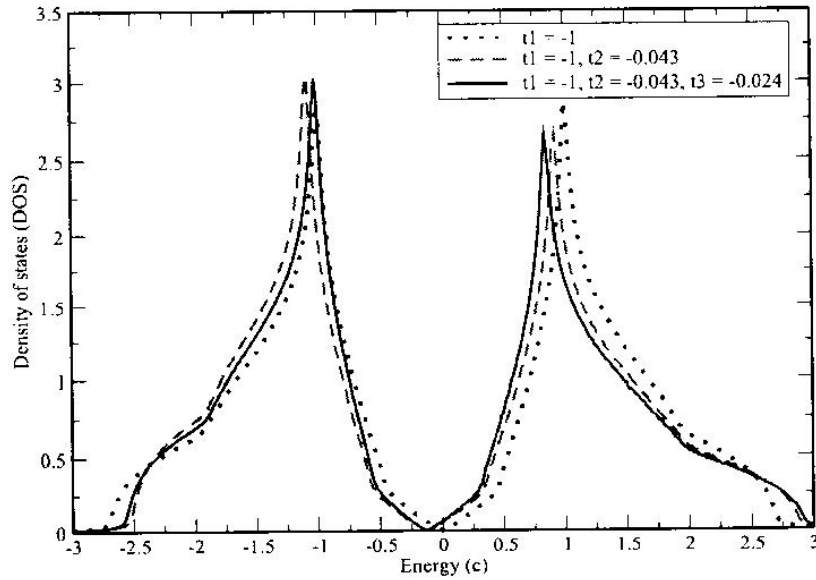


Fig. 1: shows the electronic density of states (DOS) of ideal graphene for different band energy with different hopping integrals , $\tilde{t}_1 = -1$ (solid line) for NN; $\tilde{t}_1 = -1$, $\tilde{t}_2 = -0.043$ (dotted line) for NNN , $\tilde{t}_1 = -1$, $\tilde{t}_2 = -0.043$, $\tilde{t}_3 = -0.024$ (dashed line) for NNNN.

3. Calculation

The Green's functions for the electrons of A and B sub-lattices are calculated by Zubarev's Green's function technique [38]. The pole of the Green's functions provide electron band dispersions . The density of states are calculated from the imaginary part of Green's function. Finally the occupations and their difference for sub-lattice electrons for different spin orientations are calculated to study the magnetic effect of of Coulomb interaction in the gap formation in graphene. All the energy parameters are scaled by the hopping integral t_1 .

4. Results and discussions

The band gaps can be induced in graphene near Dirac point by the following techniques

4.1 Effect of electron hopping

The electron density of states (DOS) and band dispersion are numerically computed [39] and are shown in Figs.1-2 . The tight-binding calculations give the first nearest neighbor hopping integral $t_1 = 2.5 - 3.0$ eV [25, 26] . In the present calculations we have taken $\varepsilon_a = \varepsilon_b = 0$, $t_1 = -2.78$ eV , $t_2 = -0.12$ eV , $t_3 = -0.068$ eV. Here the scaled hopping integrals become $\tilde{t}_1 = -1$, $\tilde{t}_2 = -0.043$ and $\tilde{t}_3 = -0.024$. The density of states (DOS) for electrons for the graphene is plotted for different band energies (c) [see Fig.1] . The DOS exhibits V-shaped nature at K-point (Dirac point) for nearest neighbor hopping energy $t_1 = -1$ i.e DOS shows linear dependence of band energy . When second nearest neighbor hopping ($\tilde{t}_2 = -0.043$) is included , it still retains the V-shape , but shifts to lower energies becoming asymmetric in nature with respect to Fermi level ($\varepsilon_F = 0$) at Dirac point [Fig.1]

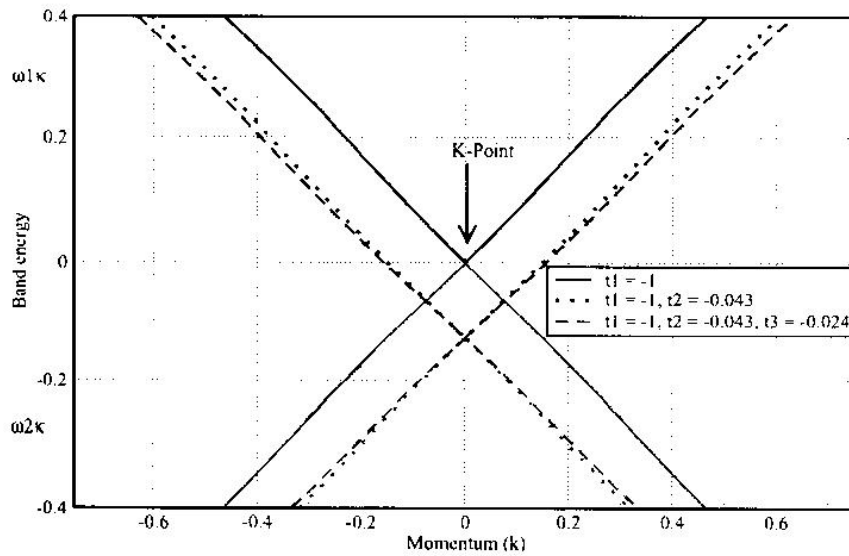


Fig. 2: shows the electronic band dispersion for ideal graphene for different band energy with different hopping integrals , $\tilde{t}_1 = -1$ (solid line) for NN ; $\tilde{t}_1 = -1$, $\tilde{t}_2 = -0.043$ (dotted line) for NNN , $\tilde{t}_1 = -1$, $\tilde{t}_2 = -0.043$, $\tilde{t}_3 = -0.024$ (dashed line) for NNNN.

The inclusion of third neighbor interaction induces a gap near K-points and the gap shifts further to lower energies. Fig. 2 shows the electron energy dispersion for the grapheme is plotted for different band hopping energy . The energy band dispersion exhibits V shaped nature at K-point (Dirac point) for nearest neighbor hopping energy $t_1 = -1$ i.e band dispersion shows linear dependence of band energy. When second nearest neighbor hopping ($\tilde{t}_2 = -0.043$) is included , it still retains the V-shape, but shifts to lower energies becoming asymmetric in nature with respect to Fermi level ($\varepsilon_F = 0$) at Dirac point [Fig.2]. The inclusion of third neighbor interaction induces a gap near K-points and the gap shifts further to lower energies .

4.2 Substrate effect

In order to study the substrate effect in band gap opening in graphene, we compute DOS and electron band dispersion near Dirac point from equation (1) and (3) [39] and show the plots in Fig.3 and Fig.4. Fig.3 shows the DOS for different values of band gaps $d_1 = 0.035$ to 0.107 arising in graphene sheet due to substrate effect [9-11, 16] and [27-29]. With the on-set of substrate effect, the Dirac point moves towards the valence band occupied by electrons and introduces a band gap below Fermi level $\varepsilon_F = 0$. The gap is further enhanced with the increase of d_1 . Fig. 4 shows the enhancement of band gap between lower electron occupied valence band and upper hole band due to the increase of d_1 . The middle of the band gap also moves down the Fermi level $\varepsilon_F = 0$.

4.3 Effect of Coulomb interaction

The sub-lattice Coulomb interaction is treated within a mean-field approximation. Using the Hamiltonian in equation (1),(3)and (4),we calculate the difference (d) in occupation numbers and modified gap $\tilde{\Delta}$ based on our earlier calculation [40].

$$d = \sum_k \frac{\tilde{\Delta} [f(\beta\omega_{1k\uparrow}) - f(\beta\omega_{2k\uparrow})]}{(\omega_{1k\uparrow} - \omega_{2k\uparrow})} \quad (7)$$

where f is the Fermi distribution function and $\omega_i = 1,2$ is the electron band dispersion. The modified gap $d_2(T) = \frac{\tilde{\Delta}}{t_1}$ is plotted in Fig. 5 and Fig. 6 for different Coulomb energy and hopping parameters. The ferromagnetic magnetizations and spin polarizations are reported [41].

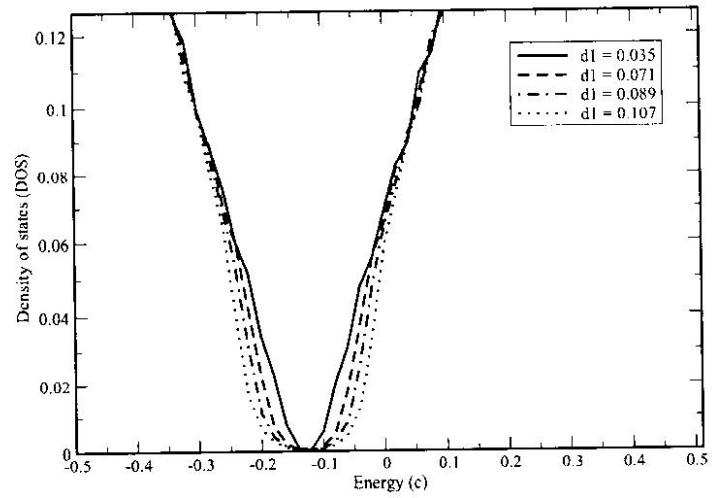


Fig. 3: shows the variation of density of states (DOS) with energy (c) for different substrates $d_1 = 0.035, 0.071, 0.089, 0.107$

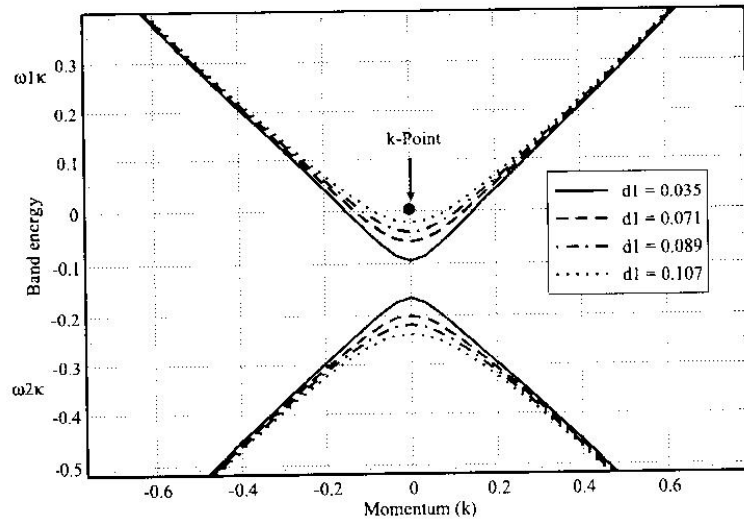


Fig. 4: shows the variation of energy band dispersion with momentum (k) for different substrates $d_1 = 0.035, 0.071, 0.089, 0.107$

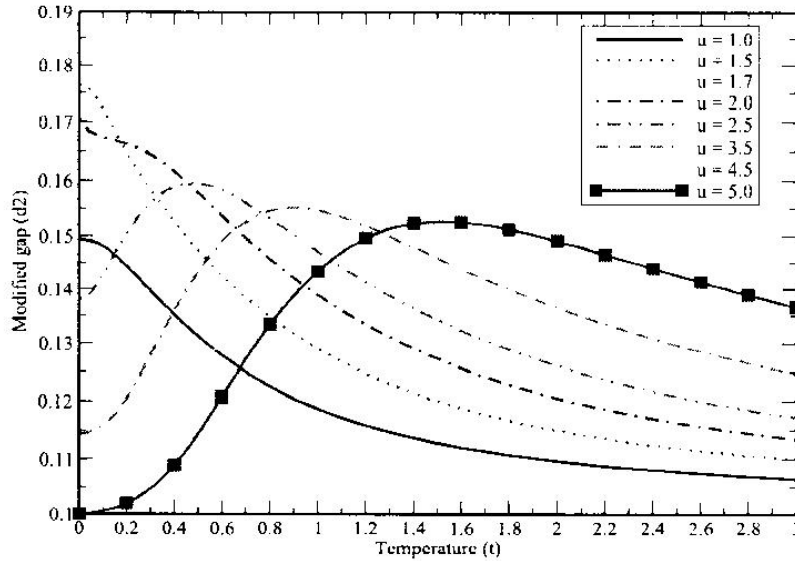


Figure 5: shows the variation of modified band gap (d_2) with temperature(t) for different values of Coulomb energy $u = 1.0, 1.5, 1.7, 2.0, 2.5, 3.5, 4.5$ and 5.0 for fixed substrate induced band gap $d_1 = 0.1$.

The graphene on-substrates acquires a band gap of Δ . The band is enhanced to

$\tilde{\Delta} = \Delta + Ud/2$ due to Coulomb interaction between electrons. When scaled by hopping integral the modified gap becomes as $d_2 = d_1 + ud/2$ using the temperature dependent difference (d) of occupancies between A and B sub-lattice up-spin electrons, the modified band gap is calculated for different Coulomb energies and the result is shown in Fig.5. For lower Coulomb energies, the modified gap (d_2) at $t = 0$ gradually increases with increase of u from 1 to 1.7 and attains the maximum of $d_2 \approx 0.182$. On further increasing to higher Coulomb energies, the modified gap (d_2) at $t = 0$ decreases and attains the bare gaps (d_1) arising due to only substrate effect for Coulomb energy $u = 5.0$. In other words the magnetic gap vanishes for $u = 5.0$ indicating that $n_{\uparrow}^a = n_{\uparrow}^b$ in paramagnetic phase. The temperature dependence of modified gap shows that the magnitude of gap for lower ' u ' gradually decreases with temperature. For higher ' u ', the modified gap increases with temperature, attains its maximum and then decreases with temperature. However the maximum of modified gap nearly remains same

for higher value of ‘ u ’ at higher temperatures indicating that $d = \langle n_{\uparrow}^a \rangle - \langle n_{\uparrow}^b \rangle$ remains unchanged at very high temperatures and Coulomb interactions.

Fig.6 shows the effect of different hopping integrals on temperature dependent modified gap (d_2). In absence of Coulomb interaction and electron hopping, the band gap in graphene is $d_1 = 0.1$ which arises due to substrate effect only. This band gap at temperature 0^0K is enhanced to $d_2 \approx 0.167$ due to the onset of a critical Coulomb energy $u_c = 1.7$ for the nearest- neighbor hopping energy of $t_1 = -1.0$. This gap at temperature 0^0K is further enhanced to $d_2 \approx 0.181$ for the same critical Coulomb energy $u_c = 1.7$ and for hopping integrals taken up to third nearest neighbor . It appears that the contributions of third nearest neighbor hopping integrals and beyond have little effect on the band gap. The temperature dependent modified gap shows that the gap is the highest at very low temperatures and gradually decreases with increase of temperature. This effects of hopping integrals on the modified gap is also seen in the band dispersions shown in the inset of the Fig.6.

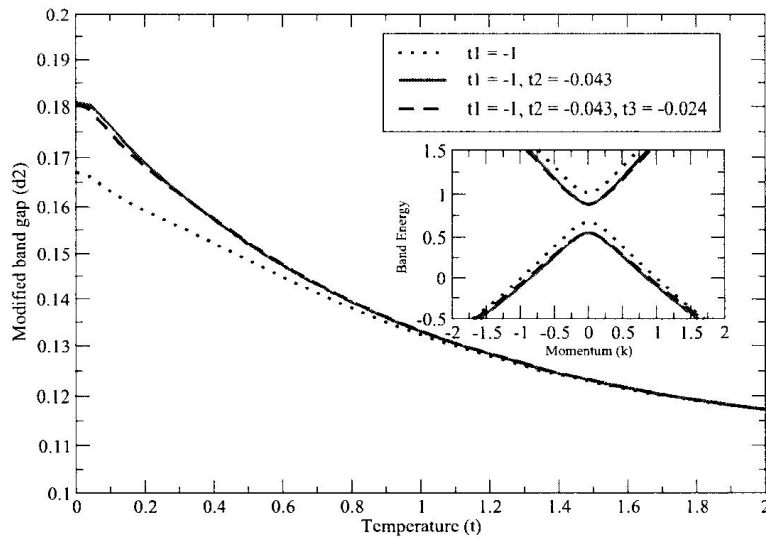


Fig. 6: shows the variation of modified band gap (d_2) with temperature(t) at $u = 1.7$ for different values of electron hopping $\tilde{t}_1 = -1$, $\tilde{t}_2 = -0.043$, $\tilde{t}_3 = -0.024$ for fixed substrate induced band gap $d_1 = 0.1$. The band dispersions for different hopping are also given in inset of the fig.

4.4 Effect of electron-phonon interaction

The electrons on graphene sheet interact strongly with the phonons on the polarized surface of substrates. Applying Lang-Firsov canonical transformation [42] to equations (1),(3),(4),(5) and (6) in high frequency limit of localized phonons, we calculate the effective Coulomb energy $\tilde{U} = (U - 2\lambda\tilde{t}_1)$ and effective hopping (\tilde{t}_1) which is a function of phonon frequency ω_0 , electron-phonon coupling (λ) and NN- hopping integral (t_1). The temperature dependent modified gaps are plotted in Fig. 7 and Fig.8.

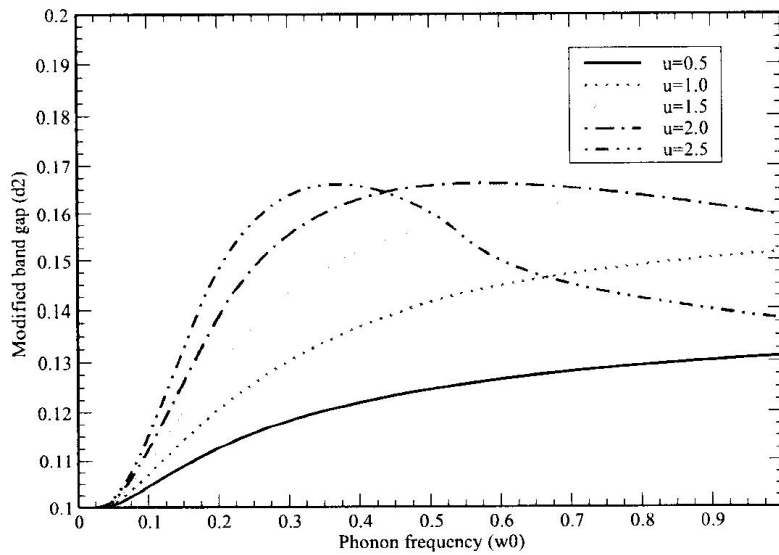


Fig. 7: Shows the variation of modified band gap (d_2) vs. phonon frequency ω_0 for different values of Coulomb potential $u = 0.5, 1.0, 1.5, 2.0, 2.5$ for fixed electron-phonon coupling constant (al) = 0.2, temperature (t) = 0.01 and substrate induced gap (d_1) = 0.1

The effect of Coulomb interaction (u) on the modified gap d_2 for high phonon frequency ω_0 vibration is shown in Fig.7. For given value of lower Coulomb interaction, the modified gap gradually increases with phonon frequency. With further increase of Coulomb energy the modified gap gradually increases from $d_1 = 0.1$ and attains maximum value $d_2 = 0.0165$ for given Coulomb interaction $u = 2.0$. With further increase in Coulomb interaction, the modified gap gradually increases with phonon frequency ω_0 attains a maximum flat peak $d_2 = 0.0165$ for critical Coulomb interaction $u_c = 2.5$ for critical phonon frequency $\omega_{0c} = 0.35$. Thus it is clear that modulated gap is maximized for critical

Coulomb interaction $u_c = 2.5$ and critical phonon frequency $\omega_{0c} = 0.35$ for given values of electron-phonon coupling $al = 0.2$. The critical Coulomb interaction $U_c = 2.5t_1$ for producing maximum modified gap is slightly higher than the critical Coulomb interaction $U_c = u_c t_1 = 1.7 t_1$ obtained earlier in the absence of electron-phonon interaction and phonon frequency [40].

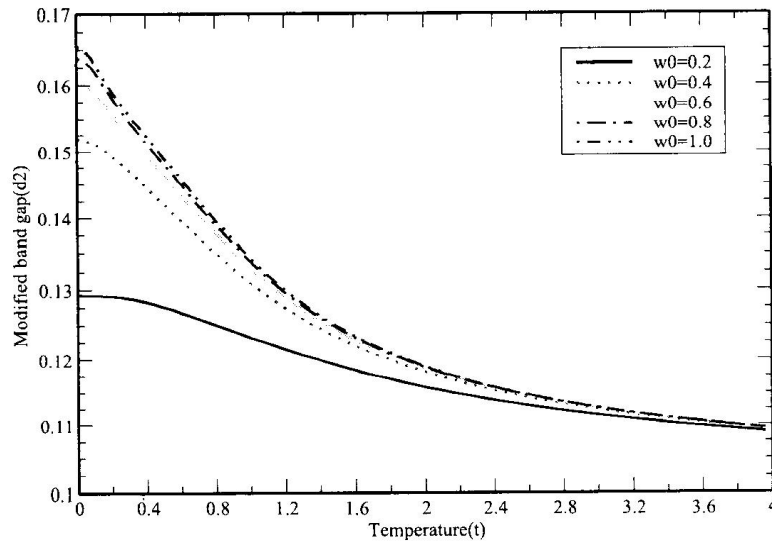


Fig. 8: Shows the variation of modified band gap (d_2) vs. temperature (t) for different values of phonon frequency (ω_0) = 0.2, 0.4, 0.6, 0.8, 1.0 for fixed electron-phonon coupling constant (al)= 0.2, Coulomb interaction (u) = 1.7 and substrate induced gap (d_1)=0.1

The effect of phonon frequency ω_0 on gap is shown in fig.8. For a given low electron-phonon coupling $al = 0.2$ and relatively low phonon frequency $\omega_0 = 0.2$, the modified $d_2 = 0.13$ gap at temperature $t = 0$. With increase of phonon vibrational frequency the modified gap is enhanced to the higher value i.e. $d_2 = 0.165$ at temperature $t = 0$ for vibrational frequency $\omega_0 = 1.0$. However, for a given phonon vibration frequency, the modified gap decreases with temperature and remains nearly constant at higher temperatures. Thus, it is clear that phonon vibrational frequency enhances the gap near room temperature.

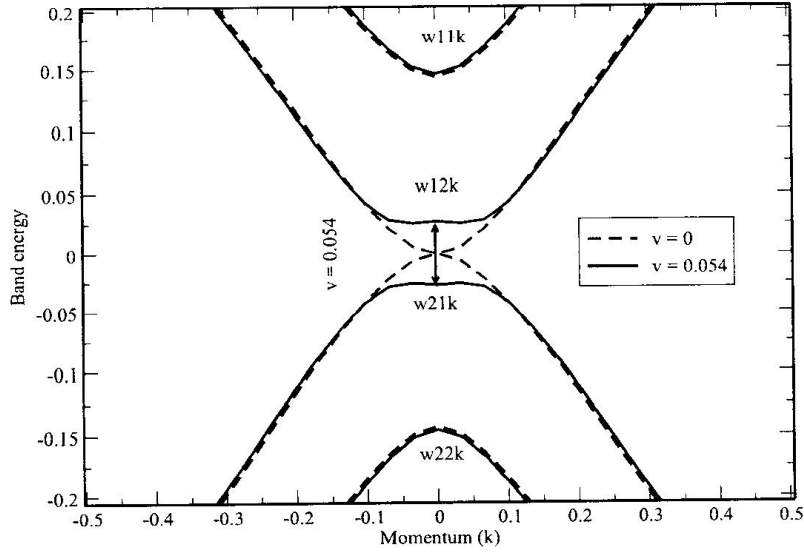


Fig. 9: shows the plot of energy band dispersions vs. momentum (k) for pristine bilayer graphene for different values of external biasing ($v = 0$ (dashed line) and $v = 0.054$ (solid line))

4.5 Effect of bilayer graphene (BLG)

Experiments [8, 17, 19] show evidence of band gap opening in graphene in BLG by gating between two layers. We have proposed model Hamiltonian consisting of intra layer and inter layer hopping integrals t_1 and t_\perp respectively in presence of gating potential V . The four bands [43] for BLG are written as

$$\omega_{\alpha,sk} = -\mu - (-1)^s \sqrt{\frac{\left[\frac{V_2}{2} + 2\varepsilon_k^2 + \varepsilon_{k\perp}^2 - (-1)^\alpha \sqrt{R} \right]}{2}} \quad (8)$$

$$R = \left[\frac{V^2}{2} + 2\varepsilon_k^2 + \varepsilon_{k\perp}^2 \right]^2 - 4 \left[\frac{V^4}{16} - \frac{\varepsilon_k^2 V^2}{2} + \frac{\varepsilon_{k\perp}^2 V^2}{4} + \varepsilon_k^4 \right] \quad (9)$$

where $s, \alpha = 1, 2$. The band dispersion is plotted in Fig. 9. which shows four bands $\omega_{\alpha,sk}$ of which ω_{11k} and ω_{22k} are high energy bands and ω_{12k} (conduction) and ω_{21k} (valence) are the low lying dispersion bands near Dirac point with zero

energy. In absence of gate potential $v = \frac{V}{t_1} = 0$ low energy bands touch at Dirac point. For low electric potential ($v = 0.054$) the low energy bands show a Mexican hat shape with a gap energy of 0.054 as observed experimentally [8, 19].

5. Conclusions

We have reported here the theoretical model calculation of band gap opening in grapheme by electron hopping, substrate effect, Coulomb interaction, electron-phonon interaction and finally formation of bilayer and multilayer graphenes. We have reported the effect of electron and hole doping on the Raman active most well known G-peak [44].

References

- [1] K S Novoselov, A. K Geim et al., *Science* **306**, 666 (2004)
- [2] K S Novoselov, A K Geim, S V Morozov and D Jiang et al., *Nature* **438**,197 (2005).
- [3] P R Wallace, *Phys. Rev.* **71**, 622 (1947).
- [4] D L Miller and K D Kubista et al., *Science* **324**, 924 (2009).
- [5] N Stander, B Huard and D Goldhaber-Gordon, *Phys. Rev. Lett.* **102**, 026807 (2009).
- [6] K I.Bolotin, K J Sikes and J Hone et al., *Phys. Rev. Lett.* **101**,096802 (2008)
- [7] M-Y Han and B Zyilmaz et al., *Phys.Rev. Lett.* **98**, 206805 (2007).
- [8] Edward McCann and Vladimir and I Falko, *Phys. Rev. Lett.* **96**, 086805 (2006).
- [9] Gianluca Giovannetti, Petr A. Khomyakov et al., *Phys. Rev. B* **76**, 073103 (2007)
- [10] S Y Zhou, G-H. Gweon, A V Fedorov and P N First et al.,*Nat. Mater.* **6** ,770 (2007)
- [11] F Varchon, R Feng and J Hass at al., *Phys. Rev. Lett.* **99** , 126805 (2007)
- [12] Alexander Mattausch and Oleg Pankratov, *Phys. Rev. Lett.* **99**, 076802 (2007).

- [13] K V Emtsev, F Speck, Th Seyller and L Ley, *Phys. Rev. B* **77**, 155303 (2008).
- [14] F Varchon, P Mallet, J -Y Veullen and L Magaud, *Phys. Rev. B* **77**, 235412 (2008)
- [15] F Varchon, P Mallet, J -Y. Veullen and L Magaud, *Phys. Rev. Lett.* **100**, 176802 (2008).
- [16] S Fratini and F Guinea, *Phys. Rev. B* **77**, 195415 (2008).
- [17] McCann, D S L Abergel and V I Falko, *Solid State Commun.* **143**, 110 (2007)
- [18] Y Zhang, T-T Tang, C Girit and Z Hao, *Nature* **459**, 820 (2009).
- [19] T Ohta, A Bostwick, T Seyller, K Horn and E Roteberg, *Science* **313**, 951 (2006).
- [20] J P Hague, *Phys. Rev. B* **84**, 155438 (2011).
- [21] J P Hague, *Phys. Rev. B* **86**, 064302 (2012).
- [22] M P Halasall and A C Ferrari, *Science* **323**,610 (2009).
- [23] P C Eklund, J O Sofo and J Zhu, *Phys. Rev. B* **81**, 205435 (2010).
- [24] L Song, L Ci and H Lu, *Nano. Lett.* **10**, 3209 (2010).
- [25] T O Wehling, E Aolu and C Friedrich, *Phys. Rev. Lett.* **106**, 236805 (2011).
- [26] V N Kotov and B Uchoa, *Rev. Mod. Phys.* **84**, 1067 (2012)
- [27] P Hansmann, T Ayrar and L Vaugier, *Phys. Rev. Lett.* **101**, 166401 (2013).
- [28] R Pariser and G Parr, *J. Chem. Phys.* **21**, 767 (1953).
- [29] Z G Soos, S Ramasesha and D S Galvo, *Phys. Rev. Lett.* **71**, 1609 (1993).
- [30] R H Friend, R W Gymer and A B Holmes, *Nature* **397**, 121 (1999).
- [31] T O Wehling, E Aolu and C Friedrich, *Phys. Rev. Lett.* **106**, 236805 (2011).
- [32] Z Y Meng, T C Lang, S Wessel, F F Assaad and A Muramatsu, *Nature* **464**, 847 (2010)
- [33] I F Herbut, *Phys. Rev. Lett.* **97**, 146401 (2006).
- [34] A H Castro Neto and F Guinea, *Rev. Mod. Phys.* **81**, 109 (2009).
- [35] J E Drut and T A Lhde, *Phys. Rev. Lett.* **102**, 026802 (2009).

- [36] S Das Sarma and S Adam, *Rev. Mod. Phys.* **83**, 407 (2011).
- [37] R G Parr, D P Craig and I G Ross, *J. Chem. Phys.* **18**, 1561 (1950).
- [38] D N Zubarev, *Sov. Phys. Usp.* **3**, 320 (1960).
- [39] S. Sahu and G C Rout, *Adv. Sci. Lett.* **20**, 834 (2014).
- [40] S Sahu and G C Rout, *Physica B* (2014) (In press)
- [41] S Sahu, S K S Parashar and G C Rout, *IJWMN* (January,9-12,2015)
(Accepted)
- [42] S Sahu, S K S Parashar and G C Rout, *Adv. Sci. Lett.* (2015)
(Communicated)
- [43] S Sahu, SKS Parashar and G C Rout, *CTCMP* (February,19-22,2015)
(Accepted)
- [44] S Sahu, S K S Parashar and G C Rout, *Nano India* (January,29-30,2015)
(Accepted)